Journal of Catalysis **194,** 393–400 (2000)
doi:10.1006/jcat.2000.2953, available online at http://www.idealibrary.com on IDEAL®

Influence of Sodium on the Structure and HDS Activity of Co–Mo Catalysts Supported on Silica and Aluminosilicate

A. M. Venezia,*,[1] F. Raimondi,† V. La Parola,† and G. Deganello*,†

*Istituto di Chimica e Tecnologia dei Prodotti Naturali del CNR (ICTPN-CNR), via Ugo la Malfa 153, 90146, Palermo, Italy; and †Dipartimento di Chimica Inorganica, Università di Palermo, Viale delle Scienze, Parco d'Ozleans, 90128, Palermo, Italy

Received February 24, 2000; revised May 29, 2000; accepted May 29, 2000

Structural changes and catalytic performances of hydrodesulfurization (HDS) Co–Mo catalysts, supported on amorphous aluminosilicate (ASA) and amorphous SiO_2 were investigated as a function of the amount of sodium ions added to the supports. The catalysts were prepared according to the incipient wet impregnation method using $(NH_4)_6Mo_7O_{24}$ as molybdenum precursor and $CoCl_2$ or $Co(NO_3)_2$ as cobalt precursor. Structural and morphological characterisations of the materials were performed with X-ray diffraction (XRD) and surface area measurements (BET). In the case of the ASA-supported catalysts, increasing the amount of sodium resulted in a gradual decrease of the catalyst surface areas and allowed formation of the β-$CoMoO_4$ phase. In the SiO_2-supported catalysts, the β-$CoMoO_4$ phase formed in the absence of sodium. Moreover, addition of the alkali ions to the amorphous silica induced the phase transition to cristobalite resulting in a drastic decrease of the surface area. The catalytic behaviour of the materials was tested in the HDS of thiophene carried out in a continuous-flow system at atmospheric pressure, in a range of temperature between 603 K and 673 K. Unlike the silica-supported catalysts that were strongly inhibited by the addition of sodium, the ASA-supported catalysts exhibited a maximum of the HDS activity in correspondence with a specific amount of sodium. A correlation between structure and activity is proposed.

Key Words: **Mo–Co catalysts; ASA and SiO_2 supports; HDS of thiophene; sodium dopant.**

1. INTRODUCTION

The hydrodesulfurization (HDS) process, used to remove sulfur from petroleum feed-stocks, is generally carried out in the presence of alumina-supported MoS_2 catalysts (1). However, most of the industrial catalysts contain cobalt which was shown to improve the catalytic activity of molybdenum (2). The promotion by Co is thought to occur through an electron transfer from the promoter to the molybdenum, reducing its oxidation state (3). It also accelerates the sulfiding of MoO_3 by supplying spillover hydrogen (4). Among the different physical models proposed for the Co–Mo HDS catalysts (1), the assumption of a Co–Mo–S structure is generally the most favoured one. Using Mossbauer spectroscopy, it was shown that the cobalt atoms are located at the MoS_2 crystallite edges forming the so-called "Co–Mo–S" structure which includes a family of structures with different Co concentrations (5). A correlation between the variation in HDS activity and the amount of Co present as Co–Mo–S was observed (5, 6). Both single- and multiple-slab Co–Mo–S structures were observed depending on the preparation and activation parameters, presence of additives, type of support, metal loading, etc. The single-slab model is called Type I and interacts more strongly with the support; the multiple-slab form, called Type II, is fully sulfided, exhibits a weak support interaction of the van der Waals type, and is considered the most active form (1, 7). The explanation for the more active nature of the Co–Mo–S sites as compared to MoS_2 or Co_9S_8 was found within the bond energy model (8) which predicts a weakening of the Mo–S bond due to a strong Co–Mo interaction. Moreover, it was shown that the metal–sulfur bond strength was lower in the Type II Co–Mo–S site. The amount of Co–Mo–S structure observed in a given catalyst is determined by the MoS_2 edge dispersion (1). Mossbauer and EXAFS spectroscopy studies showed that the local structure of Co promoter atoms in the active Co–Mo–S structure is dependent on the type of support (7, 9). Studies on the role of the support disclosed both negative and positive effects of the strong interaction between the support and the active phase of the catalysts. Alumina interacts strongly with the active phase, facilitating redispersion during operation and during regeneration (10); however, due to the strong interactions with supported Mo it favors the formation of the relatively less active Type I Co–Mo–S (1). The use of a less interacting support, like silica, tends to form the Type II Co–Mo–S; however, its superior surface acidity may induce coke formation during the HDS reactions (10, 11). Addition of secondary promoters to supported Co–Mo has been investigated aiming to affect the dispersion of the final active site (11, 13). Recently, an increase of the thiophene HDS activity was observed upon addition of a small amount of barium to alumina-supported Ni–Mo

[1] To whom correspondence should be addressed. Fax: ++39 0916809399. E-mail: anna@ictpn.pa.cnr.it.

0021-9517/00 $35.00

catalysts (14). Moreover, several patents have reported on the promotion by alkali ions of the HDS selectivity with respect to the hydrogenation of olefins (15, 16).

Co–Mo catalysts supported on amorphous aluminosilicate (ASA), and on amorphous SiO_2 previously doped with various amount of sodium ions, are here investigated. The preparation method of the two-step pore volume impregnation was adopted. Structural and morphological characterisations of the catalysts and corresponding precursors were obtained with X-ray diffraction and surface area measurements (BET). The catalytic behaviour was tested in the HDS of thiophene. The aim of the study was to find a correlation between the catalytic performance and the alkali ion-induced structural modification at the level of the oxidised precursor species.

2. EXPERIMENTAL

2.1. Supports and Catalysts Preparation

Amorphous aluminosilicate (ASA) (from Aldrich Chemical Co.) constituted of 86% SiO_2, 13% Al_2O_3, and 1% minor oxide components (surface area of 430 m^2/g, pore volume of 0.62 ml/g) and amorphous SiO_2 (from Aldrich Chemical Co. with surface area of 546 m^2/g, pore volume of 0.92 ml/g) were used as supports. A variable amount of sodium was added by incipient wetness impregnation with an aqueous solution of $NaNO_3$ of appropriate concentration. After evaporation of the water at room temperature for about 10 h, the paste was dried at 343 K for 2 h and then calcined at 773 K overnight. The obtained supports are listed in Tables 1 and 2 along with the sodium content as derived from atomic absorption spectroscopy (AAS) and with the specific surface area obtained by the nitrogen physisorption method using an automated BET apparatus.

The Mo–Co catalysts were prepared by incipient wetness impregnation. The atomic ratio Co/Mo equal to 0.4, corresponding to the best HDS activity (1), was used in all cases. The procedure involved impregnation with an $(NH_4)_6Mo_7O_{24}\cdot 4H_2O$ aqueous solution at pH 8, followed by 2 h of drying at 343 K and overnight calcination at 773 K. Thereafter the second impregnation with an aqueous solution of $CoCl_2$ or $Co(NO_3)_2$ followed by the same steps as before was carried out. The ASA-supported catalysts were prepared from both cobalt precursors; the silica-supported ones were prepared from cobalt nitrate only. The adopted sequence was chosen on the basis of previous studies showing for alumina-supported catalysts better HDS performance in the case of Mo preceding Co impregnation (17). The concentrations of Mo and Co were obtained by AAS. The catalysts, labeled according to the sodium content, are listed in Tables 3 and 4 along with their composition and specific surface areas. For comparison two catalysts without cobalt, ASA-Mo and 3.2-Na-ASA-Mo, were prepared and analysed.

TABLE 1

Sodium Content and Specific Surface Area (*S*) Measurements of the Sodium-Doped ASA Supports

Support	Wt% Na	*S* (m^2/g)
ASA	0	430
1.0-Na-ASA	1.0	380
2.0-Na-ASA	2.0	364
3.2-Na-ASA	3.2	322
4.1-Na-ASA	4.1	300
7.2-Na-ASA	7.2	74
11.7-Na-ASA	11.7	44

TABLE 2

Sodium Content and Specific Surface Area (*S*) Measurements of the Sodium-Doped SiO_2 Supports

Support	Wt% Na	*S* (m^2/g)
SiO_2	0	546
1.0-Na-SiO_2	1.0	96
2.0-Na-SiO_2	2.0	22
3.2-Na-SiO_2	3.2	25
4.1-Na-SiO_2	4.1	9
7.2-Na-SiO_2	7.2	6
11.7-Na-SiO_2	11.7	6

2.2. Structural Characterization

The X-ray diffraction measurements were performed with a Philips X-ray diffractometer using Ni-filtered Cu $K\alpha$ radiation. A proportional counter and a 0.05° step size in 2θ

TABLE 3

ASA-Supported Catalysts Composition,[a] Atomic Ratio (Na/Mo), and Specific Surface Area (*S*)

Catalyst	Wt% Na	Wt% Mo	Wt% Co	Na/Mo	*S* (m^2/g)
ASA-MoCo	0	6.4	1.6	0	266
ASA-Mo	0	6.4	0	0	390
3.2-Na-ASA-Mo	2.6	6.4	0	0	200
1.0-Na-ASA-MoCo	0.9	6.5	1.6	0.6	188
2.0-Na-ASA-MoCo	1.8	6.5	1.7	1.1	211
3.2-Na-ASA-MoCo	2.6	6.5	1.6	1.8	180
4.1-Na-ASA-MoCo	3.6	6.5	1.6	2.3	215
7.2-Na-ASA-MoCo	6.4	6.0	1.5	4.5	50
11.7-Na-ASA-MoCo	10.5	5.8	1.5	7.6	9

Note. The values refer to the samples prepared with $CoCl_2$ as cobalt precursor.

[a] The weight percentages of Na are derived from the atomic adsorption measurement values of Table 1 corrected for the increased mass due to the addition of MoO_3 and CoO.

TABLE 4

Silica-Supported Catalysts Composition,[a] Atomic Ratio (Na/Mo), and Specific Surface Area (*S*)

Catalyst	Wt% Na	Wt% Mo	Wt% Co	Na/Mo	S (m^2/g)
SiO_2-MoCo	0.0	6.6	1.3	0	450
1.0-Na-SiO_2-MoCo	1.0	6.6	1.8	0.6	69
2.0-Na-SiO_2-MoCo	2.2	6.3	1.6	1.5	14
3.2-Na-SiO_2-MoCo	3.1	6.0	1.6	2.1	18
4.1-Na-SiO_2-MoCo	4.4	6.2	1.5	3.0	7
7.2-Na-SiO_2-MoCo	7.3	6.2	1.5	4.9	2
11.7-Na-SiO_2-MoCo	11.9	6.0	1.7	8.3	1

were used. Tube voltage and current were 35 kV and 15 mA. The scanning range was between 10 and 80 2θ. The catalysts were analysed in the oxidised state, after sulfidation at 673 K for 2 h and after being used in the HDS reaction. The assignment of the various crystalline phases was based on the JPDS powder diffraction file cards (18). Information on the size of the MoS_2 crystallites was obtained from the line broadening using the Scherrer equation (19).

The microstructural characterization was performed with a Carlo Erba Sorptomat 1900 instrument. The fully computerised analysis of the adsorption isotherm of nitrogen on the samples cooled in liquid nitrogen allowed us to obtain, through the BET approach, the specific surface areas of the samples. By analysis of the desorption curve, using the Dollimore and Heal calculation method, the pore size volume distribution was also obtained (20).

2.3. Catalytic Activities

The hydrodesulfurization of thiophene was carried out in the vapour phase using a continuous-flow microreactor. An amount of 200 mg of catalyst (sieve fraction 210–430 μm), diluted with inert particles of SiC, in order to limit the radial thermal gradient, was placed inside a quartz reactor (8 mm $\emptyset$). The absence of intraparticle transport effects was checked by testing different particle sizes. Blank experiments with only the supports resulted in the complete absence of catalytic activity. Prior to the HDS measurements the catalyst was sulfided in a 50 ml/min flow of 10% H_2S in H_2, while the temperature was raised to 673 K with a heating rate of 7 K/min and kept at this temperature for 2 h. Thereafter the reactor was cooled to the reaction temperature of 603 K under flowing (30 ml/min) N_2. Meanwhile, by letting H_2 flowing through a vessel containing thiophene at 283 K, a gas mixture of 5.2 vol% of thiophene in H_2 was obtained. This mixture was let into the reactor at atmospheric pressure with a flow rate of 46 ml/min (weight hourly space velocity (WHSV) = 13,800 h^{-1}). The products were analysed by using a Carlo Erba GC 8340 gas chromatograph equipped with a packed column, 2 m long with an inner diameter of 5 mm, filled with squalene, using a flame ionization detector. The chromatogram contained peaks corresponding to the C_4 products and to thiophene. The different components of C_4 were not separated; therefore only the total C_4 signal was considered in the activity calculations. The instrumental response factors, checked experimentally, were found to be the same for the products and for thiophene within the limits of the experimental accuracy. The fractional conversion was calculated from the ratio of the peak area of the products over the sum of the peak areas of the products and thiophene. The rate constant and the specific reaction rate were calculated from the conversion under steady-state conditions. Duplicate runs were performed and the reproducibility was better than 5%. Measurements of the conversion rates at different temperatures allowed us to determine the activation energy for each catalyst. Deactivation was checked by experiments with ascending and descending temperature.

3. RESULTS

3.1. HDS Activity

Thiophene HDS conversion data were collected at 40 min interval over a period of 16 h. A plateau of steady-state conditions was reached after about 8 h. The analysis of the data was performed assuming a first-order reaction with respect to thiophene (hydrogen in large excess) and neglecting the inhibitor effect of H_2S (21). Accordingly, the reaction rate is given by the following equation,

$$r = kC_{\text{thio}}, \qquad [1]$$

where k is the rate constant and C_{thio} is the thiophene concentration. By considering

$$C_{\text{thio}} = C_0(1 - x), \qquad [2]$$

where x is the fractional conversion, C_0 is the initial thiophene concentration, and by using the integral mode of a tubular plug-flow reactor (22), k (ml g^{-1} s^{-1}) is obtained as

$$k = -\ln(1 - x)/\tau, \qquad [3]$$

where τ is the space time given by the mass of the catalysts (g) divided by the volumetric reagent gas flow F_0 (ml s^{-1}):

$$\tau = g/F_0. \qquad [4]$$

In Table 5 the catalytic activity results obtained under steady-state conditions at 603 K in terms of rate constant and specific rate (defined per grams of catalysts) are listed for all catalysts along with the activation energy calculated in the range 603–633 K. In all cases, as shown in Fig. 1 for the 3.2-Na-ASA-MoCo sample, above this temperature range deviation from the linearity in the Arrhenius plot occurred, with a distinct decrease of the activation energy at higher

TABLE 5

Catalytic Activity Results in HDS of Thiophene at 603 K

Catalyst	k (ml s^{-1} g^{-1})	r (10^{-7} mol s^{-1} g^{-1})	E_{att} (kJ/mol)
ASA-Mo	0.050	1.10	76
ASA-MoCo	0.193 (0.150)	4.05 (3.23)	85 (82)
1.0-Na-ASA-MoCo	0.377 (0.307)	7.57 (6.58)	79 (72)
2.0-Na-ASA-MoCo	0.427 (0.381)	8.64 (8.13)	86 (79)
3.2-Na-ASA-MoCo	0.397 (0.412)	8.07 (8.80)	77 (75)
4.1-Na-ASA-MoCo	0.323 (0.364)	6.53 (7.74)	79 (73)
7.2-Na-ASA-MoCo	0.015 (0.012)	0.32 (0.27)	50 (45)
11.7-Na-ASA-MoCo	0.005	0.11	N.d.[a]
3.2-Na-ASA-Mo	0.103	2.00	73
SiO_2-MoCo	0.500	9.70	73
1.0-Na-SiO_2-MoCo	0.018	0.40	41
3.2-Na-SiO_2-MoCo	0.007	0.16	35

Note. Activation energies E_{att} were calculated in the temperature range $603\,K \leq T \leq 633\,K$. The values in parentheses refer to the ASA samples prepared with $CoCl_2$ as cobalt precursor.

[a] Not determined.

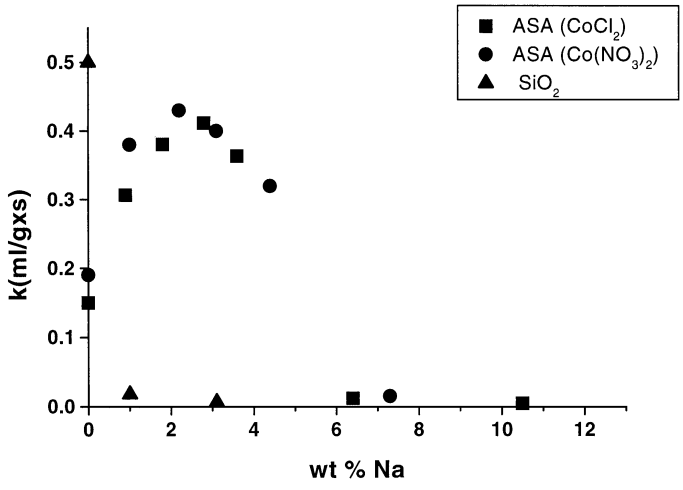

FIG. 2. Variation of the rate constant, k, versus wt% Na for the ASA- and the SiO_2-supported catalysts. Samples prepared from both cobalt precursors, $CoCl_2$ and $Co(NO_3)_2$, are included.

temperature. The dependence of the rate constant on the wt% Na is given in Fig. 2 for the MoCo catalysts. The ASA-MoCo catalysts, regardless of the cobalt precursor, exhibit a maximum activity at 3 wt% of sodium in the support. In contrast to the ASA-supported samples, the silica catalysts undergo a drastic decrease of activity upon addition of sodium.

Conversions at the beginning of the reaction were also considered in order to determine the initial deactivation. For this purpose a percentage of deactivation defined as

$$\%d = 100 \times (x_i - x_f)/x_i, \qquad [5]$$

with x_i and x_f being the conversion under the initial and stationary conditions, was calculated. The variation of $\%d$ versus wt% Na is plotted in Fig. 3 for the Mo–Co catalysts.

In all cases sodium slows down the deactivation process of the catalyst. In this respect, the catalytic behaviour of the two nonpromoted catalysts, ASA-Mo and 3.2-Na-ASA-Mo, is worth mentioning. Whereas the initial state activities were the same, the steady-state activities, given in Table 5, differ by a factor of 2 in favor of the sodium-doped sample.

3.2. Support and Catalyst Characterization

As indicated in Tables 1 and 2, addition of sodium to ASA and silica induced a decrease of the specific surface area. A relationship between the pore size distribution and the sodium content is shown in Figs. 4 and 5 where the most abundant percentages of the pores, those with sizes between 10–50 Å and between 100–300 Å versus sodium loading, are given for the two series of supports, ASA and SiO_2,

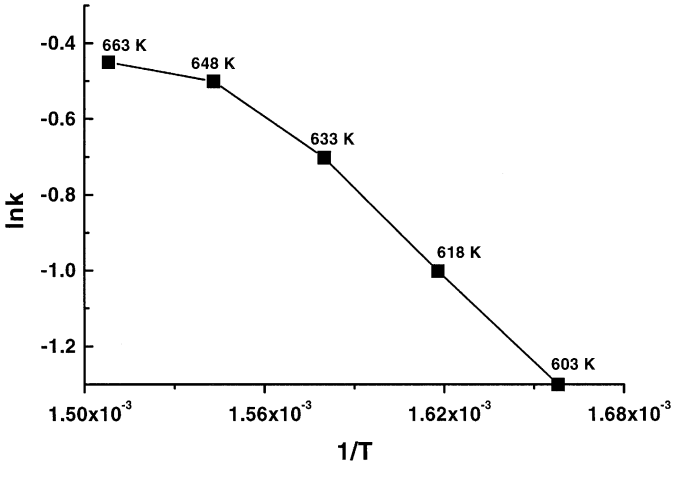

FIG. 1. Arrhenius plot for 3.2-Na-ASA-MoCo catalyst.

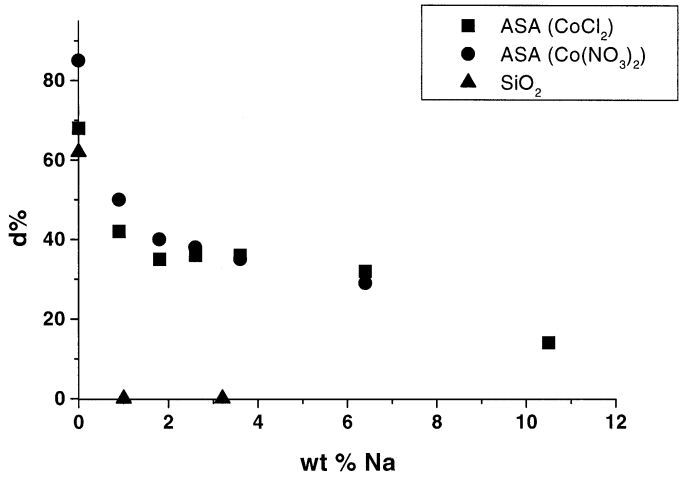

FIG. 3. Variation of the percentage of initial deactivation, d%, versus wt% Na for the ASA- and SiO_2-supported catalysts.

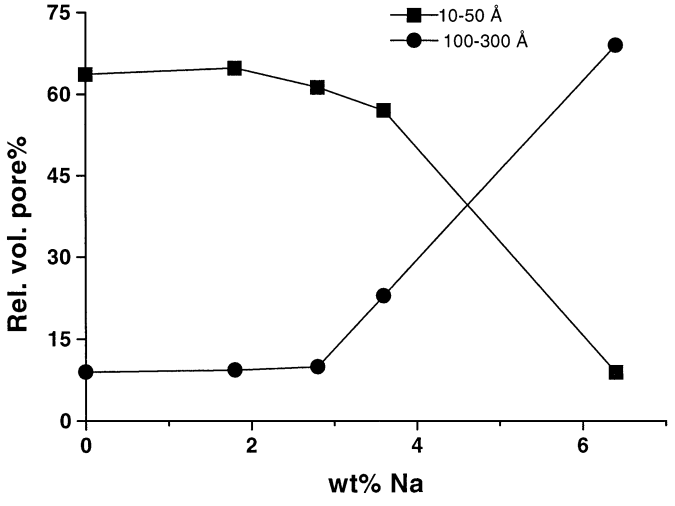

FIG. 4. Relative percentage of pores of dimension between 10–50 Å and 100–300 Å for the undoped and sodium-doped ASA supports.

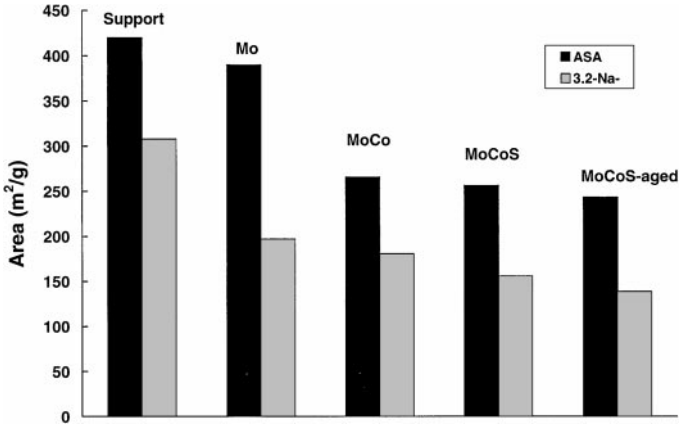

FIG. 6. Variation of the surface area with the catalyst preparation sequential steps. Two supports, ASA and 3.2-Na-ASA, are considered. The term "aged" refers to the catalyst after the HDS reaction.

respectively. In the first case, the introduction of sodium did not modify the amorphous diffractogram of the ASA, characterised by a broad feature at around $2\theta = 22^{\circ}$; an increase of the large size pores fraction occurred when the sodium loading was above 3 wt%. In the case of silica the change in pore size distribution occurred already upon addition of 1 wt% Na. As pointed out recently, sodium acts as a structural promoter by favouring the transition from amorphous silica to α-cristobalite, characterised by smaller BET surface areas, at temperatures quite below the normal transition temperature (24). As indicated by the X-ray diffractograms, shown later, such a transition becomes visible for sodium contents above 3 wt%. Plots similar to those of Figs. 4 and 5 were obtained for the corresponding calcined catalysts.

Structural changes after each step in the preparation of the ASA-supported catalysts were followed by X-ray diffraction measurements and by BET measurements. The surface area variation is shown in Fig. 6 for two supports, ASA and 3.2-Na-ASA. Most of the surface area reduction is because of the metal loading, whereas very little variation occurs upon sulfiding and after reaction. The catalyst supported on the blank ASA was amorphous as the original support. In contrast, the sodium-containing catalysts showed different crystalline phases. After Mo impregnation and subsequent calcination, $Na_2Mo_2O_7$ and Na_2MoO_4 were formed in agreement with literature (13, 23). As shown in Fig. 7 for some selected sodium-doped ASA catalysts, further loading with cobalt led to the formation of the violet β-$CoMoO_4$ (JPDS file No. 21-868) which occurred only in the presence of sodium. With increasing sodium, reflections relative to $Na_2Mo_2O_7$ and β-$CoMoO_4$ phases are observed

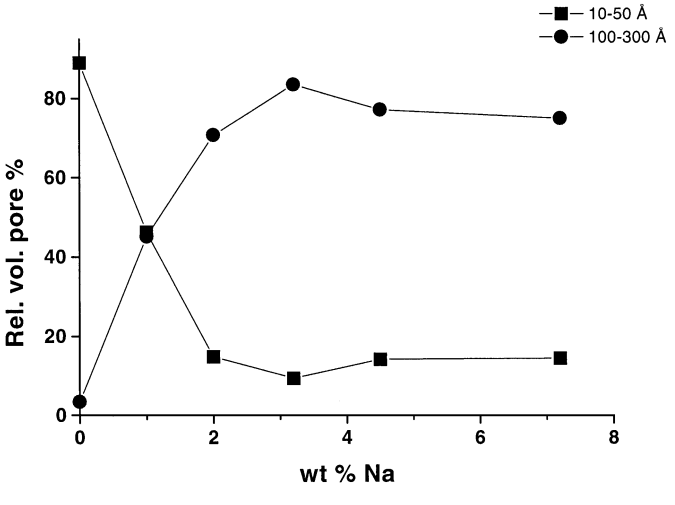

FIG. 5. Relative percentage of pores of dimension between 10–50 Å and 100–300 Å for the undoped and sodium-doped SiO_2 supports.

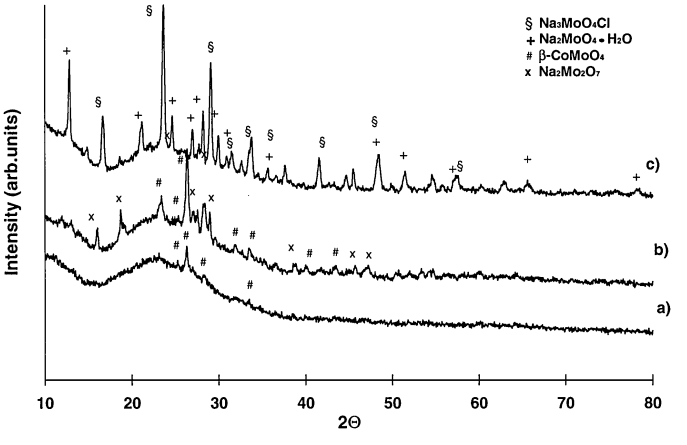

FIG. 7. Diffractograms of calcined (a) 3.2-Na-ASA-MoCo, (b) 7.2-Na-ASA-MoCo, and (c) 11.7-Na-ASA-MoCo ($CoCl_2$ was used as Co precursor).

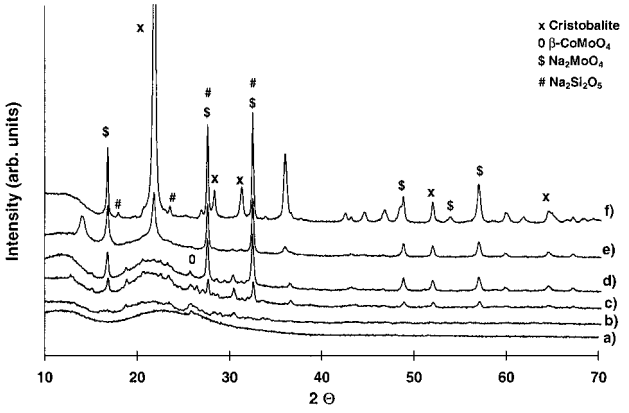

FIG. 8. Diffractograms of calcined (a) SiO_2-MoCo, (b) 1.0-Na-SiO_2-MoCo, (c) 2.0-Na-SiO_2-MoCo, (d) 3.2-Na-SiO_2-MoCo, (e) 4.1-Na-SiO_2-MoCo, and (f) 7.2-Na-SiO_2-MoCo.

(Fig. 7b). However a high sodium loading seems to decrease substantially the formation of the β-$CoMoO_4$ oxide in favor of sodium-containing phases (Fig. 7c). Quite different patterns, shown in Fig. 8, are obtained for the silica-supported catalysts. Differently from the ASA series, reflections attributable to the β-$CoMoO_4$ phase, not well crystallised, are visible also in the absence of sodium. Upon increasing the sodium content, the diffractograms of the relative samples show only sodium molybdate species. The H_2S/H_2 gas treatment at 673 K of all samples produced MoS_2 particles characterised by diffraction peaks at $2\theta = 33^\circ$ and $2\theta = 59^\circ$ indicated in Fig. 9 and attributed respectively to the (100) and (110) reflections of hexagonal structure (25). Within the limit of the XRD technique yielding average information, the absence of the MoS_2 (002) reflection in the low-angle region may suggest that, at the sulfiding temperature and pressure used, the crystalline order along the vertical axis was missing (10). This result agrees with previous work (26)

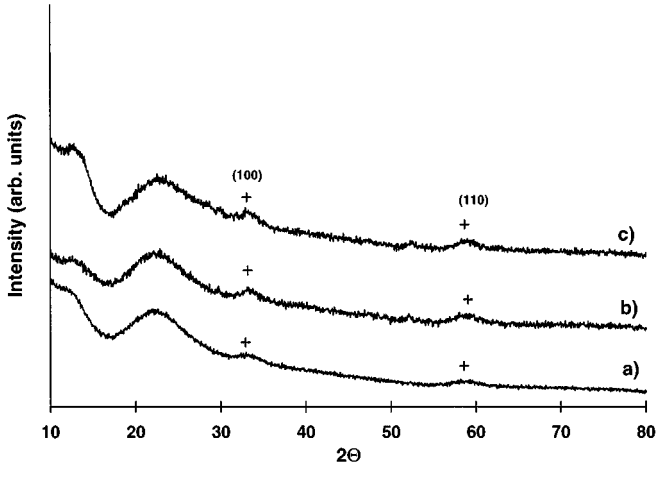

FIG. 9. Diffractograms of the sulfided (a) Asa-MoCo, (b) 3.2-Na-ASA-MoCo, and (c) 7.3-Na-ASA-MoCo.

in which the formation of tridimensional MoS_2 particles on $MoCo/Al_2O_3$ catalysts was observed only at high H_2/H_2S gas pressure. For all samples, regardless of the sodium content, the size of the particles along the basal plane, estimated from the width of the (100) reflection (19, 25), was between 60 and 80 Å. Exposure to reaction conditions did not cause a significant change of the XRD line broadening and therefore similar MoS_2 sizes were calculated.

4. DISCUSSION

The results described above indicate that the effect of Na^+ on the HDS activity of Mo–Co catalysts depended on the type of support. In the case of aluminosilicate, the addition of the alkali ions promoted the HDS activity up to a sodium loading of 4 wt%, exhibiting a maximum at around 3 wt% Na. Such behaviour occurred under initial as well as stationary conditions. In contrast, the addition of sodium to silica resulted in a brusque decrease of the HDS activity of the supported Mo–Co catalysts. The contradiction with a previous study, which concluded that Na completely depressed the HDS activity of similar catalysts supported on aluminosilicate (11), was only apparent since that study referred to samples in which the additive ions were impregnated on the finished Co–Mo catalysts; with the same impregnation procedure as used here, only a catalyst containing 5 wt% Na was investigated (11).

The diffractograms of the sulfided catalysts were all similar, and could not explain the different catalytic behaviour between the two series of samples. In contrast, the structures of the oxidised catalysts were affected differently by the presence of sodium. As evidenced by the diffractograms of the sodium-doped ASA-supported catalysts, addition of sodium in amounts between 1 wt% and 7 wt% resulted in the formation of the β-$CoMoO_4$ phase. In analogy with what was observed in alumina-supported catalysts (27), although to a small degree, because we are dealing with an aluminosilicate (28), the absence of β-$CoMoO_4$ in the undoped ASA-MoCo catalyst could also be attributed to the stronger interaction between the individual metals and the support as compared to the interaction between Co and Mo (27). Na^+, by suppressing the ASA support acidity through the decrease of the OH groups (29), and therefore decreasing its interaction with the supported elements, may allow for the formation of the β-$CoMoO_4$ species. From the enhanced reducibility of the Co^{2+} in sodium-doped Co-Mo-Al_2O_3 catalysts, the formation of β-$CoMoO_4$ was previously attributed to the presence of sodium (30). Contradictory statements exist about the importance of this species. Some authors reported that β-$CoMoO_4$ formation during the calcination step leads to the inactive Co_9S_8 (31). Other studies considered this intermediate oxide as a precursor to the active CoMoS Type II phase (1, 32). Indeed both species, the oxidised and the sulfided, are characterised by Mo in

tetrahedral coordination and Co in octahedral coordination (5, 32). In this respect, it seems plausible to attribute the presently observed effect of sodium to the formation of the β-$CoMoO_4$ leading to the active CoMoS phase. This is also supported by the improved catalytic behaviour of the 3.2-Na-ASA-MoCo with respect to the 3.2-Na-ASA-Mo catalyst. Different from the ASA catalysts, sodium is not needed to form the precursor β-$CoMoO_4$ species in the silica-supported samples.

In both series, the presence of sodium affects the initial catalyst deactivation. As shown in Fig. 3, the percent deactivation decreased with sodium, drastically in the silica-supported samples and gradually in the aluminosilicate-supported catalysts. Generally speaking, deactivation is caused either by coke formation, strictly related to the acidity of the support, or by sintering of the active phase, both factors leading to a diminished number of available catalytic sites (1, 33). On the basis of the invariance of the MoS_2 particle dimension, and the slight reduction of surface area (Fig. 6), significant sintering of the catalyst during the reaction may not have occurred. Therefore, it is likely that the main reason for the initial catalyst deactivation arises from coke deposition. As mentioned before, the alkali ions would neutralise the acidity of the support, therefore decreasing the formation of coke (15). Moreover, a comparison of the initial deactivation plot (Fig. 3) and the variation of the pore size distribution with sodium content, shown in Figs. 4 and 5 for the ASA and SiO_2 supports, respectively, indicates that the catalysts which deactivated less contained the largest fraction of large pores which were not likely to be clogged by coke. The higher HDS activity, under stationary conditions, of the 3.2-Na-ASA-Mo as compared to the activity of ASA-Mo catalyst (Table 5) can also be attributed to reduction of catalyst deactivation.

Additional information on the possible structural effect of sodium could be obtained from the experimental activation energies listed in Table 5. Small variations of their values are ascribable to experimental uncertainty. However, overall, it can be stated that the samples with the lowest catalytic activities have the lowest activation energy. A decrease in this quantity is observed for all catalysts above 633 K (Fig. 1). Assuming a Langmuir–Hinshelwood model for the HDS reaction of thiophene, the measured activation energy, E^{app}, does not correspond to the real activation energy of the rate-limiting surface reaction step, E^{rls}, but is closely related to it by the following equation,

$$E^{app} = E^{rls} + (1 - \theta)\Delta H_{ads}, \qquad [6]$$

with θ denoting the surface coverage by thiophene and ΔH_{ads} representing the heat of adsorption of thiophene. At low temperatures when the coverage is close to 1, the two values coincide; at high temperatures the coverage decreases and therefore a decrease of the measured activation energy is usually observed (34). In some cases, however, such variation is ascribed to different catalytic sites being activated at different temperatures (35). In the present study, assuming that the real activation energy for the process is the same for all catalysts, and therefore that the catalytic sites are similar, the low E^{app} values found for the lowest activity catalysts, which contain the largest amount of sodium, could be attributed to a decrease of the thiophene surface coverage caused by sodium.

In conclusion, addition of a certain amount of sodium ions to the ASA support of Mo–Co catalysts, although causing a slight decrease of the support surface area, favours the formation of the active-phase precursor, β-$CoMoO_4$, and therefore is beneficial for the HDS activity. The consequent reduction of the support acidity decreases the initial deactivation likely caused by coke. However, an excess of sodium is detrimental for the activity due to excessive covering of the active sites. Different behaviour occurs in the silica-supported catalysts, where the formation of the active-phase precursor, β-$CoMoO_4$, does not require the presence of sodium. Moreover, the surface area decreases noticeably as a result of the sodium driven transition from amorphous SiO_2 to α-cristobalite. Consequently, no positive effect whatsoever arises from sodium addition but only structural changes leading to sintering of the surface area.

5. CONCLUSION

The present study indicates that sodium ions added to the aluminosilicate support of MoCo catalysts play a role in determining the activity, under initial and stationary conditions, of the HDS reaction of thiophene. The increase of HDS activity with increasing sodium up to 3.2 wt% may be associated with the promoted formation of β-$CoMoO_4$, a likely precursor of the active CoMoS phase. In the silica-supported catalysts, the formation of such phase does not require the presence of sodium which, by causing the amorphous cristobalite phase transition, lowers the surface area. By comparing the activation energies for the HDS reaction on the sulfided catalysts, the decline of activity with a large amount of sodium is ascribed to a decrease of the surface coverage by thiophene. For all catalysts sodium is beneficial for the decrease of the initial deactivation.

ACKNOWLEDGMENTS

The authors acknowledge a grant for the "Progetto Finalizzato M.S.T.A.-II." The assistance of Mr. A. Mezzapica and Mr. N. Mondello for arranging the reaction line is gratefully acknowledged.

REFERENCES

1. Topsoe, H., Clausen, B. S., and Massoth, F. E., *in* "Hydrotreating Catalysis" (J. R. Anderson and M. Boudart, Eds.). Springer, Berlin, 1996.
2. Massoth, F. E., *J. Catal.* **30**, 204 (1973).
3. Harris, S., and Chianelli, R. R., *J. Catal.* **98**, 17 (1986).

4. Iwamoto, R., Inamura, K., Nozaki, T., and Lino, A., *Appl. Catal. A* **163**, 217 (1997).
5. Wivel, C., Clausen, R., Clausen, B. S., Morup, S., and Topsoe, H., *J. Catal.* **68**, 783 (1981).
6. Koranyi, T. I., and Paal, Z., *Appl. Surf. Sci.* **52**, 141 (1991).
7. Bouwens, S. M. A. M., van Zon, F. B. M., van Dijk, M. P., van der Kraan, A. M., De Beer, V. H. J., van Veen, J. A. R., and Koningsberger, D. C., *J. Catal.* **146**, 375 (1994).
8. Norskov, J. K., Clausen, B. S., and Topsoe, H., *Catal. Lett.* **13**, 1 (1992).
9. Bouwens, S. M. A. M., van Veen, J. A. R., Koningsberger, D. C., de Beer, V. H. J., van Veen, J. A. R., and Prins, R., *J. Phys. Chem.* **95**, 123 (1991).
10. Breysse, M., Portefaix, J. L., and Vrinat, M., *Catal Today* **10**, 489 (1991).
11. Muralidhar, G., Massoth, F. E., and Shabtai, J. J., *J. Catal.* **85**, 44 (1984).
12. Lycourghiotis, A., Defosse, C., Delannay, F., Lemaitre, J., and Delmon, B., *J. Chem. Soc., Faraday Trans. 1* **76**, 1677 (1980).
13. Lycourghiotis, A., Defosse, C., Delannay, F., and Delmon, B., *J. Chem. Soc., Faraday Trans. 1* **76**, 2052 (1980).
14. Olorunyolemi, T., and Kydd, R. A., *Catal. Lett.* **59**, 27 (1999).
15. Hatanaka, S., Sadakane, O., Hikita, S., and Miyama, T., U.S. Patent 5,853,579, 1998.
16. Sudhakar, C., U.S. Patent 5,770,046, 1998.
17. Breysse, M., Bennett, B. A., Chadwick, D., and Vrinat, M., *Bull. Soc. Chim. Belg.* **90**, 1271 (1981).
18. "JCPDS Powder Diffraction File." Int. Centre for Diffraction Data, Swarthmore, PA, 1989.
19. Klug, H. P., and Alexander, L. E., "X-Ray Diffraction Procedures for Polycrystalline and Amorphous Materials," 2nd ed., pp. 688, 704. Wiley, New York, 1974.
20. Gregg, S. J., and Sing, K. S. W., "Adsorption, Surface Area and Porosity," 2nd ed. Academic Press, San Diego, 1982.
21. Scheffer, B., Arnoldy, P., and Moulijn, J. A., *J. Catal.* **112**, 516 (1988).
22. Anderson, J. R., and Pratt, K. C., "Introduction to Characterization and Testing of Catalysts," p. 203. Academic Press, Australia, 1985.
23. Banares, M. A., Spencer, N. D., Jones, M. D., and Wachs, I. E., *J. Catal.* **146**, 4 (1994).
24. Palermo, A., Vazquez, J. P. H., Lee, A. F., Tikhov, M. S., and Lambert, R. M., *J. Catal.* **177**, 259 (1998).
25. Sullivan, D. L., and Ekerdt, J., *J. Catal.* **172**, 64 (1997).
26. Pollack, S. S., Makowsky, L. E., and Brown, F. R., *J. Catal.* **59**, 452 (1979).
27. Okamoto, Y., Imanaka, T., and Teranishi, S., *J. Catal.* **65**, 448 (1980).
28. Navarro, R., Pawlec, B., Fierro, J. L. G., Vasudevan, P. T., Cambra, J. F., and Arias, P. L., *Appl. Catal. A* **137**, 269 (1996).
29. Ivanov, V. A., Pieplu, A., Lavalley, J. C., and Nortier, P., *Appl. Catal. A* **131**, 323 (1995).
30. Ramaswamy, A. V., Sivasanker, S., and Ratnasamy, P., *J. Catal.* **42**, 107 (1976).
31. van Veen, J. A. R., Gerkema, E., van der Kraan, A. M., Hendriks, P. A. J. M., and Beens, H., *J. Catal.* **133**, 112 (1992).
32. Brito, J. I., and Barbosa, A. L., *J. Catal.* **171**, 467 (1997).
33. Furimsky, E., and Massoth, F. E., *Catal. Today* **52**, 381 (1999).
34. Hensen, E. J. M., Vissenberg, M. J., de Beer, V. H. J., van Veen, J. A. R., and van Santen, R. A., *J. Catal.* **163**, 429 (1996).
35. Leliveld, R. G., van Dillen, A. J., Geus, J. W., and Koningsberger, D. C., *J. Catal.* **175**, 108 (1998).